Metal Ion Extraction/Insertion Reactions with Todorokite-Type Manganese Oxide in the Aqueous Phase

Qi Feng*

Faculty of Science, Kochi University, 2-5-1 Akebono-cho Kochi-shi 780, Japan

Hirofumi Kanoh, Yoshitaka Miyai, and Kenta Ooi*

Shikoku National Industrial Research Institute, 2217-14 Hayashi-cho Takamatsu-shi 761-03, Japan

Received May 2, 1995. Revised Manuscript Received July 13, 1995[⊗]

Todorokite-type magnesium manganese oxide (ToMO(Mg)) was prepared by hydrothermal treatment of Mg^{2+}-exchanged buserite-type manganese oxide. The extraction/insertion reactions of the metal ions with the manganese oxide were investigated by chemical and X-ray analyses, FT-IR spectroscopy, pH titration, and K_d measurements. Mg^{2+} and Mn^{2+} ions in the (3 × 3) tunnel sites of the manganese oxide were topotactically extracted by acid treatment. Alkali metal ions could be inserted into the (3 × 3) tunnel sites of the acid-treated sample (ToMO(H)). The extraction reaction proceeded by redox-type and ion-exchange-type mechanism, and most of the insertion reaction by ion-exchange-type mechanism. In the pH titration studies, the acid-treated sample showed dibasic acid behavior toward Li^+, Na^+, and K^+ but monobasic acid behavior toward Cs^+ and $(CH_3)_4N^+$. The affinity order was $(CH_3)_4N^+ < Cs^+ = Li^+ < Na^+ < K^+$ at pH 5 and $(CH_3)_4N^+ < Cs^+ < K^+ < Na^+ < Li^+$ at pH 10. The distribution coefficient (K_d) of the metal ions increased with an increase in the effective ionic radius. The effective pore radius of ToMO(H) was evaluated as about 2.7 Å from the structural parameters of the (3 × 3) tunnel.

Introduction

Todorokite-type manganese oxide has a one-dimensional (3 × 3) tunnel structure, as shown in Figure 1. Monovalent and bivalent metal ions and water molecules generally occupy the (3 × 3) tunnel sites.[1–5] Although todorokite-type manganese oxide occurs in nature, natural todorokite-type manganese oxide of high purity is rare. Golden et al. have reported a synthetic todorokite-type manganese oxide which was prepared by hydrothermal treatment of Mg^{2+}-exchanged birnessite.[6,7] Recently, Shen et al. have developed a thermally stable todorokite-type manganese oxide[8,9] and found it can be used as a molecular sieve with a pore size of 6.9 Å. The magnetic and electrochemical properties of the manganese oxide have been also studied.[10,11] However, the metal ion adsorptive properties for the todorokite-type manganese oxides have not yet been clarified.

Manganese oxides with tunnel and layered structures show ion-sieve properties for the adsorption of metal ions. Spinel-type manganese oxides with a three-dimensional (1 × 3) tunnel structure show a specific high selectivity for the adsorption of Li^+ among alkali, alkaline-earth, and transition-metal ions.[12–25] Hollan-

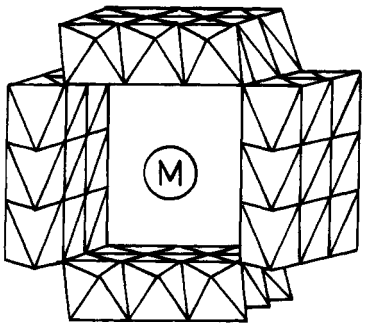

Figure 1. Structure of todorokite-type manganese oxide. The MnO_6 octahedra link together, sharing edges to form the (3 × 3) tunnel structure.

[⊗] Abstract published in *Advance ACS Abstracts,* August 15, 1995.
(1) Turner, S.; Buseck, P. *Science* **1981,** *212,* 1024.
(2) Burns, R. G.; Burns, V. M. *Manganese Dioxide Symposium*; Tokyo, Cleveland, OH; Vol. 2, 1980, p 97.
(3) Burns, R. G.; Burns, V. M.; Stockman, H. W. *Am. Mineral.* **1985,** *70,* 205.
(4) Post, J. E.; Bish, D. L. *Am. Mineral.* **1988,** *73,* 861.
(5) Giovanoli, R. *Am. Mineral.* **1985,** *70,* 202.
(6) Golden, D. C.; Chen, C. C.; Dixon, J. B. *Science* **1986,** *231,* 717.
(7) Golden, D. C.; Chen, C. C.; Dixon, J. B. *Clays Clay Minerals* **1987,** *35,* 271.
(8) Shen, Y. F.; Zerger, R. P.; Suib, S. L.; McCurdy, L.; Potter, D. I.; O'Young, C. L. *J. Chem. Soc., Chem. Commun.* **1992,** *17,* 1213.
(9) Shen, Y. F.; Zerger, R. P.; DeGuzman, R. N.; Suib, S. L.; McCurdy, L.; Potter, D. I.; O'Young, C. L. *Science* **1993,** *260,* 511.
(10) Suib, S. L.; Iton, L. E. *Chem. Mater.* **1994,** *6,* 429.
(11) DeGuzman, R. N.; Shen, Y. F.; Shaw, B. R.; Suib, S. L.; O'Young, C. L. *Chem. Mater.* **1993,** *5,* 1395.
(12) Ooi, K.; Miyai, Y.; Katoh, S. *Sep. Sci. Technol.* **1987,** *22,* 1779.
(13) Shen, X. M.; Clearfield, A. *J. Solid State Chem.* **1986,** *64,* 270.
(14) Vol'khin, V. V.; Leont'eva, G. V.; Onolin, S. A. *Neorg. Mater.* **1973,** *6,* 1041.
(15) Leont'eva, G. V.; Chirkova, L. G. *Zh. Prikl. Khin.* **1988,** *61,* 734.
(16) Ooi, K.; Miyai, Y.; Katoh, S. *Sep. Sci. Technol.* **1986,** *21,* 755.
(17) Ooi, K.; Miyai, Y.; Katoh, S. *Solvent Extr. Ion Exch.* **1987,** *5,* 561.
(18) Ooi, K.; Miyai, Y.; Katoh, S.; Maeda, H.; Abe, M. *Bull. Chem. Soc. Jpn.* **1988,** *61,* 407.
(19) Miyai, Y.; Ooi, K.; Katoh, S. *J. Colloid Interface Sci.* **1989,** *130,* 5251.
(20) Ooi, K.; Miyai, Y.; Katoh, S.; Maeda, H.; Abe, M. *Langmuir* **1989,** *5,* 150.
(21) Ooi, K.; Miyai, Y.; Sakakihara, J. *Langmuir* **1991,** *7,* 1167.
(22) Feng, Q.; Miyai, Y.; Kanoh, H.; Ooi, K. *Langmuir* **1992,** *8,* 1861.
(23) Feng, Q.; Miyai, Y.; Kanoh, H.; Ooi, K. *Chem. Mater.* **1993,** *5,* 311.

0897-4756/95/2807-1722$09.00/0

dite- or cryptomelane-type manganese oxides with a one-dimensional (2 × 2) tunnel structure show a specific high selectivity for the adsorption of metal ions with an effective ionic radius of about 1.4 Å, e.g., K^+, Rb^+, and, Ba^{2+}.[12,26-29] Birnessite-type manganese oxide with a layered structure of 7.2 Å basal spacing shows a specific high selectivity for the adsorption of Rb^+ among alkali-metal ions.[30] Manganese oxide with a layered structure of 7.4 Å basal spacing shows the highest selectivity for the adsorption of Cs^+ among alkali-metal ions.[31] The selective properties can be explained on the basis of the ion-sieve effect of the tunnel and layered structures. The (1 × 3) tunnel of the spinel structure is suitable in size for fixing Li^+,[12-18] the (2 × 2) tunnel of the hollandite structure is suitable in size for fixing metal ions with an effective ionic radius of about 1.4 Å,[26-29] and the interlayer space of the birnessite is suitable in size for fixing metal ions with an effective ionic radius of about 1.5 Å.[30]

Manganese oxide with the tunnel or layered structure can be obtained by topotactically extracting alkali- or alkaline-earth metal ions from a corresponding manganese oxide containing these ions using an acid treatment.[12-28,30-32] Our studies of the metal ion extraction/insertion reactions with the manganese oxides have indicated that the reactions proceed by redox-type and ion-exchange-type reactions.[20-24,29] The proportions of the redox-type and ion-exchange-type reactions are dependent on the oxidation state of manganese.[19-22,29]

The present paper describes a fundamental study of metal ion extraction/insertion reactions with a todorokite-type manganese oxide that was prepared by our newly developed method.

Experimental Section

Sample Preparation. Na^+-form buserite (BuMO(Na)) was prepared by pouring a mixed solution (100 mL) of 1 M H_2O_2 and 0.5 M NaOH into a solution (50 mL) of 0.3 M $Mn(NO_3)_2$ with stirring. After reaction for 1 h, the precipitate (BuMO(Na)) was filtered and washed with water. BuMo(Na) (10 g) was immersed in a solution (1 L) of 1 M $MgCl_2$ with stirring for 1 day. The sample was filtered and washed with water. The Mg^{2+}-exchanged buserite (BuMO(Mg)) was obtained by treating BuMO(Na) with $MgCl_2$ three times. BuMO(Mg) (10 g) and water (80 mL) were placed in a Teflon-lined, sealed, stainless steel vessel (110 mL) and autoclaved at 140 °C under autogenous pressure for 2 days to obtain todorokite-type magnesium manganese oxide (ToMO(Mg)). The vessel was cooled to room temperature, and the suspension was filtered, washed with water, and air-dried at room temperature for 3 days.

Metal Ion Extraction/Insertion Reactions. Metal ion extraction and insertion with ToMO(Mg) were investigated at room temperature. In the extraction study, ToMO(Mg) (10 g) was immersed in a 1 M nitric acid solution (1 L) for 2 days. The acid treatment was repeated three times to obtain an acid-treated sample (ToMO(H)). In the insertion study, ToMO(H) (1 g) was immersed in a 1 M MOH (M = Li, Na, K, or Cs) solution (100 mL) for 7 days to obtain the alkali-metal ion inserted sample (ToMO(Li), ToMO(Na), ToMO(K), or ToMO(Cs)). The extracted and inserted samples were filtered, washed with water, and air-dried at room temperature for 3 days.

Chemical Analysis. The available oxygen of each sample was determined by the standard oxalic acid method as described previously.[22] The mean oxidation number (Z_{Mn}) of manganese was evaluated from the value of available oxygen. The lithium, sodium, potassium, cesium, magnesium, and manganese contents were determined after dissolving the sample in a mixed solution of H_2SO_4 and H_2O_2. Lithium, sodium, potassium, cesium, and magnesium concentrations were determined by atomic absorption spectrometry. Manganese concentration was determined by absorption spectrometry at 523 nm after oxidizing Mn to Mn(VII) with $(NH_4)_2S_2O_8$.

Physical Analysis. An X-ray analysis was carried out using a Rigaku type RINT1200 X-ray diffractometer with a graphite monochromator. Any mechanical deviation of diffraction angles was corrected by scanning the whole angle range with silicon powder. Infrared spectra were obtained by the KBr method on a JEOL Model JTR-RFX3001 infrared spectrometer. DTA-TG curves were obtained on a MAC Science thermal analyzer (System 001, TG-DTA 2000) at a heating rate of 10 °C/min. The water content of the samples was calculated from the weight loss of the TG curve in a temperature range 30–400 °C.

pH Titration. A 0.1-g portion of each acid-treated sample was immersed in a mixed solution (10 mL) of MCl + MOH (M = Li, Na, K, Cs, $(CH_3)_4N$) in varying ratios with intermittent shaking at 25 °C. The concentration of MCl was adjusted to 0.1 M. After the sample was shaken for 7 days, the pH of the supernatant solution was determined with a Horiba Model M8s pH meter.

Distribution Coefficient (K_d). K_d values of alkali- and alkaline-earth metal ions were determined by a batch method. A 0.1-g portion of ToMO(H) sample was immersed in 10 mL of a solution containing 10^{-3} M each of Li^+, Na^+, K^+, Rb^+, and Cs^+ or a solution containing 5×10^{-4} M each of Mg^{2+}, Ca^{2+}, Sr^{2+}, and Ba^{2+} at different pH values. The pH values were adjusted using a HNO_3 solution. After attaining equilibration (14 days), the metal ion concentrations in the solution were determined by atomic absorption spectrometry. The metal ion uptake was calculated from the concentration relative to the initial concentration in the solution. The K_d value was calculated using the following equation:

$$K_d\,(\text{mL/g}) = \frac{\text{metal ion uptake (mmol/g of sample)}}{\text{metal ion concentration (mmol/mL solution)}}$$

Results and Discussion

Preparation and Characterization of Todorokite-Type Magnesium Manganese Oxide. The X-ray diffraction patterns of BuMO(Na), BuMO(Mg), and ToMO(Mg) are shown in Figure 2. BuMO(Na) prepared by reacting Mn^{2+} with H_2O_2 in a NaOH solution has a layered structure with a basal spacing of 10.04 Å in a wetted state. The basal spacing changed to 7.2 Å after air-drying at room temperature. The layered structure of BuMO(Na) remained after Mg^{2+}-exchange. BuMO(Mg) has a basal spacing of 9.68 Å. BuMO(Mg) transformed to the todorokite structure by hydrothermal treatment at 140 °C. The major difference in the X-ray pattern between ToMO(Mg) and BuMO(Mg) is the relative intensity of the peaks at d values of 9.64 and 4.76 Å. The X-ray diffraction pattern of ToMO(Mg) shows major peaks at d values of 9.64, 4.76, 3.16, 2.45, 2.40, and 2.14 Å; most of the peaks are in agreement with those in the literature.[6,7,9,33] This indicates that ToMO(Mg) has a (3 × 3) tunnel structure which belongs

(24) Liu, Y. F.; Feng, Q.; Ooi, K. *J. Colloid Interface Sci.* **1994**, *163*, 130.
(25) Feng, Q.; Kanoh, H.; Miyai, Y.; Ooi, K. *Chem. Mater.*, in press.
(26) Tsuji, M.; Abe, M. *Solv. Extr. Ion Exch.* **1984**, *2*, 253.
(27) Tsuji, M.; Abe, M. *Bull. Chem. Soc. Jpn.* **1985**, *58*, 1109.
(28) Tsuji, M.; Komarneni, S. *J. Mater. Res.* **1993**, *8*, 611.
(29) Feng, Q.; Kanoh, H.; Miyai, Y.; Ooi, K. *Chem. Mater.* **1995**, *7*, 148.
(30) Feng, Q.; Kanoh, H.; Miyai, Y.; Ooi, K. *Chem. Mater.*, in press.
(31) Tsuji, M.; Komarneni, S.; Tamaura, Y.; Abe, M. *Mater. Res. Bull.* **1992**, *27*, 741.
(32) Hunter, J. C. *J. Solid State Chem.* **1981**, *39*, 142.

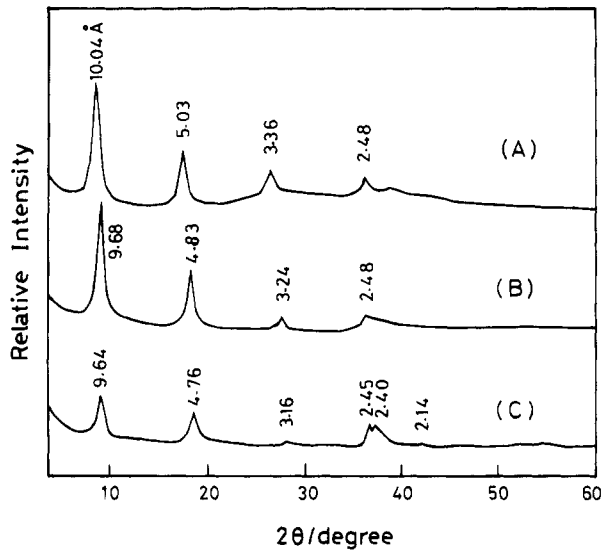

Figure 2. X-ray diffraction patterns of prepared manganese oxide samples. (A) BuMO(Na); (B) BuMO(Mg); (C) ToMO(Mg).

to a monoclinic system (space group $P2/m$).[4,33] The lattice constants are a = 9.7 Å, b = 2.8 Å, c = 9.6 Å, and β = 95°.

The buserite structure with a basal spacing of about 10 Å contains two-dimensional sheets of edge-shared MnO_6 octahedra, with double-crystal water sheets between the sheets of edge-shared MnO_6 octahedra and a Na^+ or Mg^{2+} sheet between the crystal water sheets.[1,2,10] Since hydration of Na^+ with the crystal water is weak, the crystal waters in BuMO(Na) are easily lost, thus transforming the buserite structure to birnessite structure (basal spacing 7.2 Å) after drying. The birnessite structure has a single-crystal water sheet between the MnO_6 octahedral sheets.[2,34] The Mg^{2+}-exchanged buserite keeps the double water sheet structure due to the strong hydration effect of Mg^{2+} with the crystal water. Since the size of the hydrated Mg^{2+} just fits the (3 × 3) tunnel of the todorokite structure, the BuMO(Mg) is transformed to the todorokite structure by the hydrothermal treatment.[6]

IR spectra of BuMO(Na), BuMO(Mg), and ToMO(Mg) are shown in Figure 3. In the spectrum of BuMO(Na) (Figure 3A), the bands at 3430 cm^{-1} and the band at 1650 cm^{-1} can be assigned to stretching and bending vibrations of the −OH group of crystal and adsorbed water molecules, respectively. The bands in the region from 400 to 800 cm^{-1} can be assigned to Mn−O stretching vibrations.[2,13,23] In the spectrum of BuMO(Mg) (Figure 3B), the presence of two bands at 3400 and 3210 cm^{-1} indicates the presence of two kinds of crystal water. The bands in the region from 400 to 800 cm^{-1} of ToMO(Mg) (Figure 3C) can be assigned to Mn−O and Mg−O stretching vibrations, and these bands are in agreement with the bands of todorokite-type manganese oxides in the literature.[6,7] This suggests that the buserite structure was transformed to the todorokite structure by the hydrothermal treatment. The band around 3220 cm^{-1} (Figure 3C) can be assigned to stretching vibration of the −OH group of crystal water molecules.

(33) $NaMn_6O_{12}\cdot 3H_2O$ (ASTM 38-0475).
(34) Hirano, S.; Narita, R.; Naka, S. *Mater. Res. Bull.* **1984**, *19*, 1229.

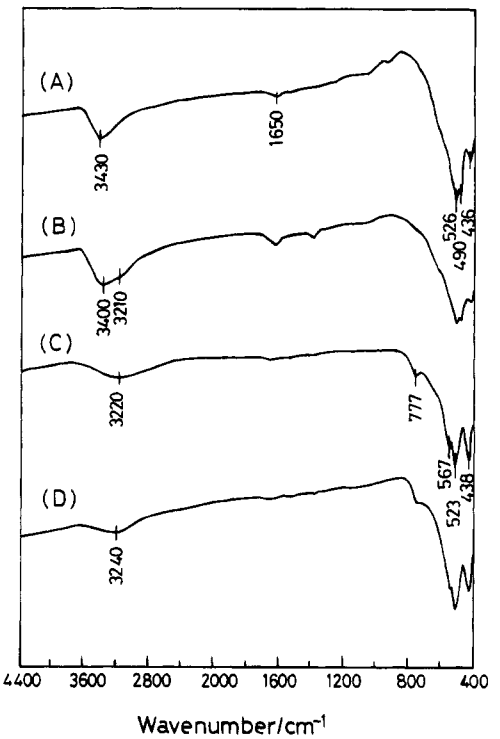

Figure 3. IR spectra of prepared and acid-treated manganese oxide samples. (A) BuMO(Na); (B) BuMO(Mg); (C) ToMO(Mg); (D) ToMO(H).

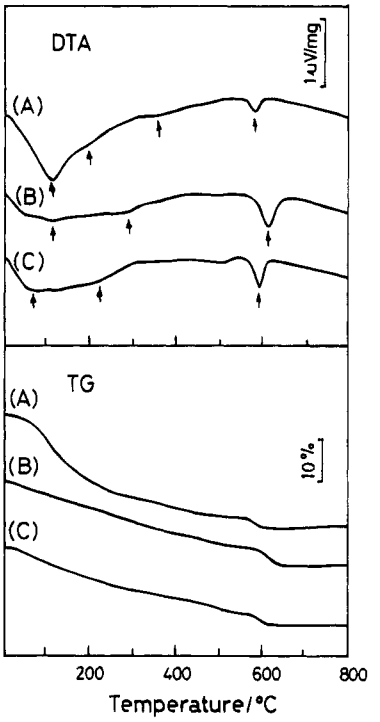

Figure 4. DTA (top) and TG (bottom) curves for prepared and acid-treated manganese oxide samples. (A) BuMO(Mg); (B) ToMO(Mg); (C) ToMO(H).

DTA-TG curves for BuMO(Mg) and ToMO(Mg) are shown in Figure 4. BuMO(Mg) showed an endothermic peak at 118 °C and shoulders at 203 and 352 °C, each with a weight loss (Figure 4A). The peak and shoulders correspond to the dehydration of the crystal waters. The endothermic peak at 587 °C with a weight loss corresponds to the transformation of Mn(IV) to Mn(III) with the release of oxygen. In the DTA-TG curves for ToMO-

Table 1. Composition of Prepared Manganese Oxides[a]

sample	Z_{Mn}	M/Mn	H_2O/Mn
BuMO(Na)	3.71	0.339	0.62
BuMO(Mg)	3.76	0.112	1.3
ToMO(Mg)	3.71	0.113	0.71

[a] M: Na, Mg.

Table 2. Composition and Formula of Acid-Treated and Alkali-Metal Ion Inserted Samples[a]

sample	Z_{Mn}	M/Mn	Mg/Mn	H_2O/Mn	formula
ToMO(H)	3.93		0.052	0.68	$\{H_{1.1}\}[Mg_{0.3}Mn_{5.7}]O_{12}\cdot 3.3H_2O$
ToMO(Li)	3.90	0.187	0.051	0.87	$\{Li_{1.1}H_{0.1}\}[Mg_{0.3}Mn_{5.7}]O_{12}\cdot 4.9H_2O$
ToMO(Na)	3.91	0.162	0.051	0.72	$\{Na_{0.9}H_{0.2}\}[Mg_{0.3}Mn_{5.7}]O_{12}\cdot 4.0H_2O$
ToMO(K)	3.91	0.147	0.051	0.66	$\{K_{0.8}H_{0.3}\}[Mg_{0.3}Mn_{5.7}]O_{12}\cdot 3.6H_2O$
ToMO(Cs)	3.91	0.093	0.050	0.60	$\{Cs_{0.5}H_{0.6}\}[Mg_{0.3}Mn_{5.7}]O_{12}\cdot 3.1H_2O$

[a] M: Li, Na, K, Cs.

(Mg) (Figure 4B), endothermic shoulders around 122 and 286 °C weight losses correspond to the dehydration of the crystal waters. The endothermic peak at 616 °C with a weight loss corresponds to the transformation of Mn(IV) to Mn(III) with the release of oxygen. An X-ray diffraction study indicated that the todorokite structure remains until 400 °C.

Compositional analysis results for samples BuMO-(Na), BuMO(Mg), and ToMO(Mg) are summarized in Table 1. 99% of the Na^+ in BuMO(Na) was removed by the $MgCl_2$ treatment. The mean oxidation numbers (Z_{Mn}) of Mn and the Mg/Mn mole ratio were almost constant before and after the hydrothermal treatment, but the water content decreased, in agreement with the results of IR spectra. The compositional formula of ToMO(Mg) can be written as $Mg_{0.7}Mn_{6.1}O_{12}\cdot 4.3H_2O$. The Mg/Mn mole ratio and the mean oxidation number (Z_{Mn}) of Mn for ToMO(Mg) (Table 1) are different from the todorokite-type manganese oxides prepared by Golden et al. (0.163 and 3.79)[6] or Shen et al. (0.151−0.215 and 3.39−3.41).[8] This indicates that the composition of todorokite-type manganese oxide varies slightly depending on preparation method or conditions.

Characterization of Acid-Treated Samples. When ToMO(Mg) was treated with a 1 M HNO_3 solution, 60% of the Mg^{2+} was extracted from the solid, and 9.4% of the Mn was dissolved. The compositional analysis result for the acid-treated sample (ToMO(H)) is shown in Table 2. The mean oxidation number (Z_{Mn}) of Mn increased after the acid treatment, owing to a disproportionation reaction of Mn(III) to Mn(IV) and Mn(II) in the acid solution[22,28,32] and the extraction of Mn^{2+} from the tunnel sites. The water content decreased after the extraction of Mg^{2+}.

The X-ray diffraction pattern of ToMO(H) shows that the todorokite structure remained after the acid treatment (Figure 5A). The acid treatment causes a slight change in the lattice constants a and β (a = 9.6 Å, b = 2.8 Å, c = 9.6 Å, and β = 94°). This indicates that the extraction reactions proceed topotactically, maintaining the todorokite structure. In the IR spectrum of ToMO-(H) (Figure 3D), the vibration bands corresponding to the todorokite structure in the region 400−800 cm^{-1} remained. The band around 3240 cm^{-1} can be assigned to stretching vibrations of the −OH group of crystal water molecules and the lattice −OH groups or H_3O^+ which are formed by Mg^{2+}/H^+ and Mn^{2+}/H^+ ion-exchange reactions occuring in the acid-treatment process. DTA-TG curves for ToMO(H) showed endothermic

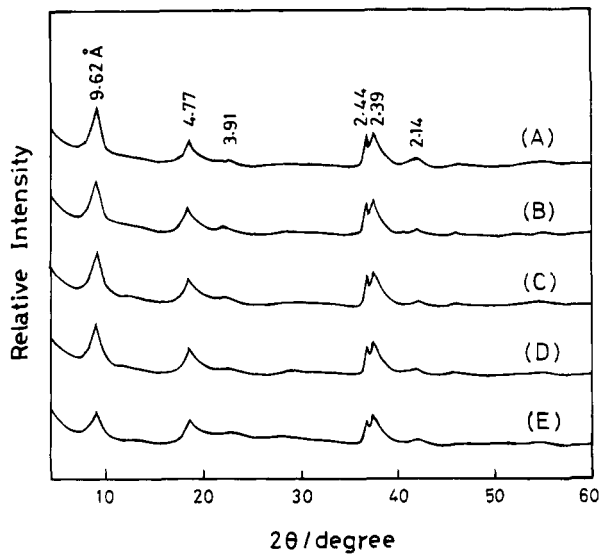

Figure 5. X-ray diffraction patterns of the acid-treated and alkali-metal-ion inserted samples. From top: (A) ToMO(H); (B) ToMO(Li); (C) ToMO(Na); (D) ToMO(K); (E) ToMO(Cs).

shoulders around 76 and 220 °C with weight losses (Figure 4C). These shoulders can be attributed to the dehydration of the crystal water and dissipation of water by condensation of the lattice −OH group. The lattice −OH groups are formed by Mg^{2+}/H^+ and Mn^{2+}/H^+ ion-exchange reactions. The endothermic peak at 595 °C with a weight loss corresponds to the transformation of Mn(IV) to Mn(III).

Model for the Extraction Reaction. We think that the formula for an idealized todorokite-type magnesium manganese oxide can be written as eq 1, in which only

$$\{Mg_x\}[Mn^{III}_{2x}Mn^{IV}_{6-2x}]O_{12} \quad (1)$$

Mg^{2+} occupy the (3 × 3) tunnel sites, where { } and [ ] are (3 × 3) tunnel sites and octahedral sites of the todorokite framework, respectively, the $x \leq 1$. The crystal water molecule was omitted for simplicity, although, in actual fact, hydrated Mg^{2+} occupy the tunnel sites.

Since only 60% of Mg^{2+} can be extracted from ToMO-(Mg) by the acid treatment, there may be two types of Mg^{2+} in the ToMO(Mg). One occupies the (3 × 3) tunnel sites and the other the octahedral sites. The Mg^{2+} in the tunnel sites can be extracted easily by the acid treatment since they are hydrated ions, but Mg^{2+} in the octahedral sites may not be so easily extracted. In addition, the hydrated Mn^{2+} can also occupy the (3 × 3) tunnel sites.

The formula of actual todorokite-type magnesium manganese oxide can be written as follows:

$$\{Mg_xMn^{II}_y\}[Mg_zMn^{III}_nMn^{IV}_{6-z-n}]O_{12} \quad (2)$$

where $x + y \leq 1$, $z \leq 1$, and $n \leq 1$. When the fraction of Mg^{2+} extracted by the acid treatment is assumed to be equal to the fraction of Mg^{2+} in the tunnel sites, the parameters x, y, z, and n can be evaluated from the chemical analysis data in Table 1 as follows:

$$x/(x + z) = 0.6 \quad (3)$$

$$(x + z)/(y + 6 - z) = (Mg/Mn) \quad (4)$$

$$\{2y + 3n + 4(6 - z - n)\}/(y + 6 - z) = Z_{Mn} \quad (5)$$

$$2(x + y + z) + 3n + 4(6 - z - n) = 24 \quad (6)$$

The formula of ToMO(Mg) can be written as follows:

$$\{Mg_{0.4}Mn^{II}{}_{0.4}\}[Mg_{0.3}Mn^{III}{}_{1.0}Mn^{IV}{}_{4.7}]O_{12} \quad (7)$$

As with ToMO(Mg), the formula for ToMO(H) can be evaluated from the chemical analysis data in Table 2 as follows:

$$\{H_{1.1}\}[Mg_{0.3}Mn^{III}{}_{0.5}Mn^{IV}{}_{5.2}]O_{12} \quad (8)$$

where all Mg^{2+} and Mn^{2+} in the tunnel sites are assumed to be extracted by the acid treatment. The H^+ in the tunnel sites are formed by Mg^{2+}/H^+ or Mn^{2+}/H^+ ion-exchange reaction, but the H^+ content is less than the equivalent amount of Mg^{2+} and Mn^{2+} in the tunnel sites. The Mn(III) content in the octahedral site is decreased, while the Mn(IV) content is increased by the acid treatment.

The change in the chemical formula due to the acid treatment can be well explained by considering redox-type reactions. Similar to the case of the spinel-, hollandite-, and birnessite-type manganese oxides,[21,22,29,30] a redox-type reaction occurs in the metal ion extraction process in addition to the ion-exchange-type reaction. The redox-type extraction of one Mg^{2+} or Mn^{2+} in the tunnel sites accompanies the disproportionation of two Mn(III) to Mn(IV) and Mn(II). The Mn(IV) remains in the solid phase, and Mn(II) dissolves into the solution phase. Since the extraction reactions are a one-phase solid solution reaction,[21,22,29] the extraction reaction can be described as

$$\{Mg_{0.4}Mn^{II}{}_{0.4}\}[Mg_{0.3}Mn^{III}{}_{1.0}Mn^{IV}{}_{4.7}]O_{12} + 2.11H^+ \rightarrow 0.96\{H_{1.1}\}[Mg_{0.3}Mn^{III}{}_{0.5}Mn^{IV}{}_{5.2}]O_{12} + 0.41Mg^{2+} + 0.65Mn^{2+} + 0.53H_2O \quad (9)$$

Equation 9 shows that 31% and 69% of the metal ions in the tunnel sites are extracted by the redox-type reaction and the Mg^{2+}/H^+ or Mn^{2+}/H^+ ion-exchange-type reaction, respectively.

Metal Ion Insertion Reaction. Structural and compositional studies were carried out on the alkali-metal ion inserted samples. The X-ray patterns of the alkali-metal ion inserted samples (ToMO(Li), ToMO(Na), ToMO(K), and ToMO(Cs)) show that the todorokite structure remained after the metal ion insertions (Figure 5). This indicates that the metal ion insertion reactions proceed topotactically. The change in the intensity of diffraction peaks for the alkali-metal ion inserted samples suggests that the metal ions entered into the lattice of the todorokite-type manganese oxide. The relatively large change for ToMO(Cs) may be due to the large X-ray scattering ability of inserted Cs^+.

The results of the compositional analysis of the metal ion inserted samples are given in Table 2. The formulas for these samples which can be evaluated from the compositional analysis data are also given in Table 2. The alkali-metal content and water content increase in the order $Cs^+ < K^+ < Na^+ < Li^+$, in agreement with the decreasing order of the ionic radii. The Mg/Mn mole ratios are almost constant before and after the insertion reactions, indicating the Mg^{2+} in the octahedral sites of the todorokite framework are ion-exchange inert. The high alkali-metal contents indicate that the metal ions entered into the bulk crystal. The formulas of metal ion inserted samples suggest that all the (3 × 3) tunnel sites are occupied by Li^+ and half of the sites by Cs^+. This can be understood by comparing the diameters of Li^+ (1.36 Å) and Cs^+ (3.34 Å) with the lattice constant b (2.8 Å) of ToMO(H) and considering steric effect of these metal ions.

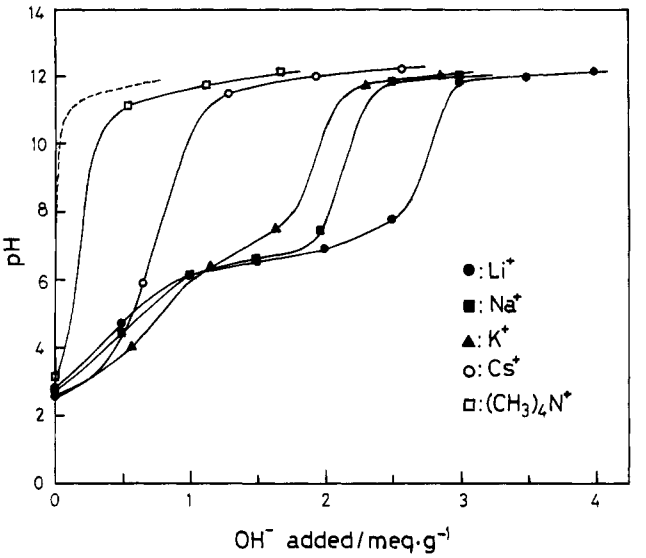

Figure 6. pH titration curves of ToMO(H): sample, 0.1 g; solution, 0.1 M MCl + MOH (M = Li, Na, K, Cs or $(CH_3)_4N$); total volume of solution, 10 mL; temperature, 20 °C; (- - -) blank titration.

The insertion reactions caused slight decreases in the Z_{Mn} values (Table 2). A small amount of O_2 evolution gas and Mn(VII) coloring were observed in the solution during the Li^+ insertion. These facts suggest the presence of a small amount of redox-type reaction during the metal ion insertions. Redox-type insertion reactions were also observed in the alkali-metal ion insertion reactions with spinel-, hollandite-, and birnessite-type manganese oxides.[20-22,29,30] Most of the alkali-metal ion insertion reactions are ion-exchange-type reactions, in which alkali-metal ions substitute for the H^+ or H_3O^+ in the tunnel sites.

pH Titration. The pH titration curves of the acid-treated sample ToMO(H) in (0.1 M ACl + AOH, A = Li, Na, K, Cs and $(CH_3)_4N$) solutions are shown in Figure 6. ToMO(H) showed dibasic acid behavior toward Li^+, Na^+, and K^+, and monobasic acid behavior toward Cs^+ and $((CH_3)_4N)^+$. This indicates that there are two types of sites for the adsorption of alkali metal ions. The apparent capacity of ToMO(H) for Li^+, Na^+, K^+, and Cs^+ increases in the order $Li^+ = Cs^+ < Na^+ < K^+$ at pH < 5. This suggests that the stronger acidic site, dissociating below pH 5, is suitable for the adsorption of K^+. Hollandite-type manganese oxide has also shown a similar affinity sequence in this acidic region.[26,29] The capacity sequence changes to $Cs^+ < K^+ < Na^+ < Li^+$ in the range of pH > 10; the sequence agrees with the decreasing order of the effective ionic radii of metal ions. The weaker acidic site, dissociating above pH 6, is suitable for small ions, owing to a steric effect in a state of high metal ion loading. Cs^+, which has a large ionic radius, can be adsorbed only on the stronger acidic sites.

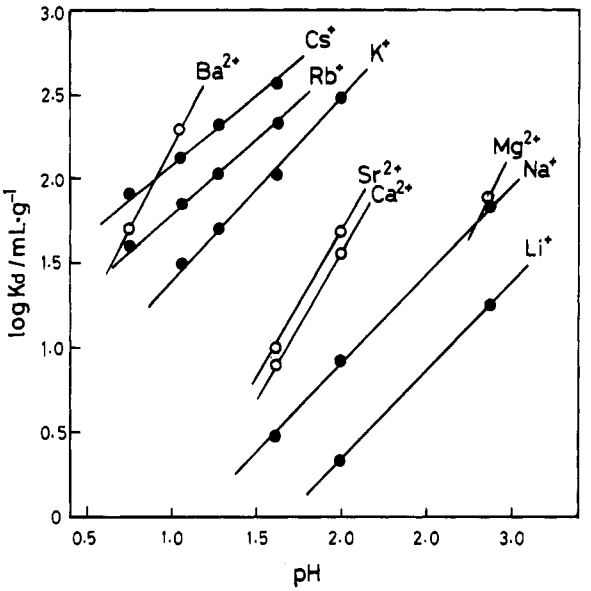

Figure 7. Plots of the distribution coefficients (K_d) of alkali- and alkaline-earth-metal ions on the ToMO(H) against solution pH.

The apparent capacity (about 0.3 mmol/g) for $(CH_3)_4N^+$ is remarkably smaller than that for the alkali-metal ions over the pH range studied. This is due to the ion-sieve effect of the (3 × 3) tunnel site. The $(CH_3)_4N^+$ cannot enter the (3 × 3) tunnel sites, owing to their ionic radii being too large (3.5 Å);[35] they can exchange only with the protons of the surface −OH group. On the other hand, the alkali-metal ions can exchange not only with the protons of the surface −OH group but also with those in the (3 × 3) tunnel sites.

Selectivity of Alkali- and Alkaline-Earth-Metal Ions. The equilibrium K_d values of alkali- and alkaline-earth-metal ions on ToMO(H) are plotted as a function of solution pH in Figure 7. The logarithms of the K_d values increase linearly with increasing pH over the pH range studied. The slopes of d log K_d/d pH can be approximated to 1 for alkali-metal ions and 2 for alkaline-earth-metal ions. The selectivity sequence is $Li^+ < Na^+ < K^+ < Rb^+ < Cs^+$ for alkali-metal ions, and $Mg^{2+} < Ca^{2+} < Sr^{2+} < Ba^{2+}$ for alkaline-earth-metal ions over the pH range studied. The sequences are in agreement with the increasing order of the effective ionic radii of metal ions. This suggests that alkali- and alkaline-earth-metal ions can enter the (3 × 3) tunnel sites in the todorokite structure without steric effect, owing to the large tunnel size. A plot of log K_d against the effective ionic radius of the alkali metal ion[36] is shown in Figure 8. ToMO(H) does not show a maximum value of K_d in the region of the effective ionic radius of the alkali-metal ion, since the effective pore radius of ToMO(H) is larger than the effective ionic radius of Cs^+. The effective pore radius of ToMO(H) can be evaluated as about 2.7 Å from the structural parameters of ToMO-(H) by comparing it with the effective pore radius and the structure parameters of hollandite-type manganese oxide with (2 × 2) tunnel structure.[29]

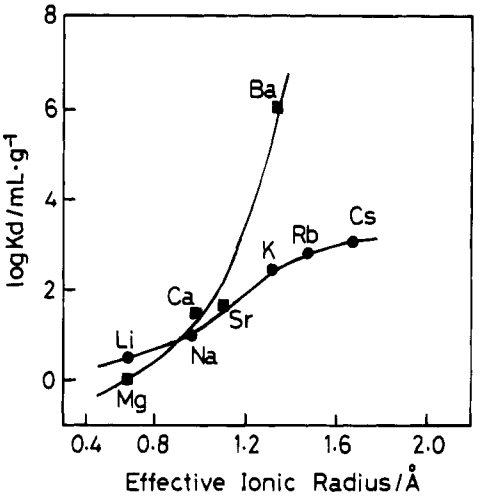

Figure 8. Distribution coefficients (K_d) of alkali- and alkaline-earth-metal ions on the ToMO(H) at pH 2 as a function of effective ionic radius.[36]

Conclusions

Todorokite-type magnesium manganese oxide can be prepared by hydrothermal treatment of Mg^{2+}-exchanged buserite-type manganese oxide. Mg^{2+} and Mn^{2+} in the (3 × 3) tunnel sites can be topotactically extracted from the magnesium manganese oxide by acid treatment. The acid-treated sample shows ion-sieve properties for the adsorption of cations. The effective pore radius of ToMO(H) is about 2.7 Å.

CM950201F

(35) Robinson, R. A.; Stokes, R. H. *Electrolyte Solutions*; Academic Press: New York, 1959.

(36) Shannon, R. D.; Prewitt, C. T. *Acta Crystallogr.* **1969**, *B25*, 925.